Cell

Monoclonal 1- and 3-Phosphohistidine Antibodies: New Tools to Study Histidine Phosphorylation

Graphical Abstract

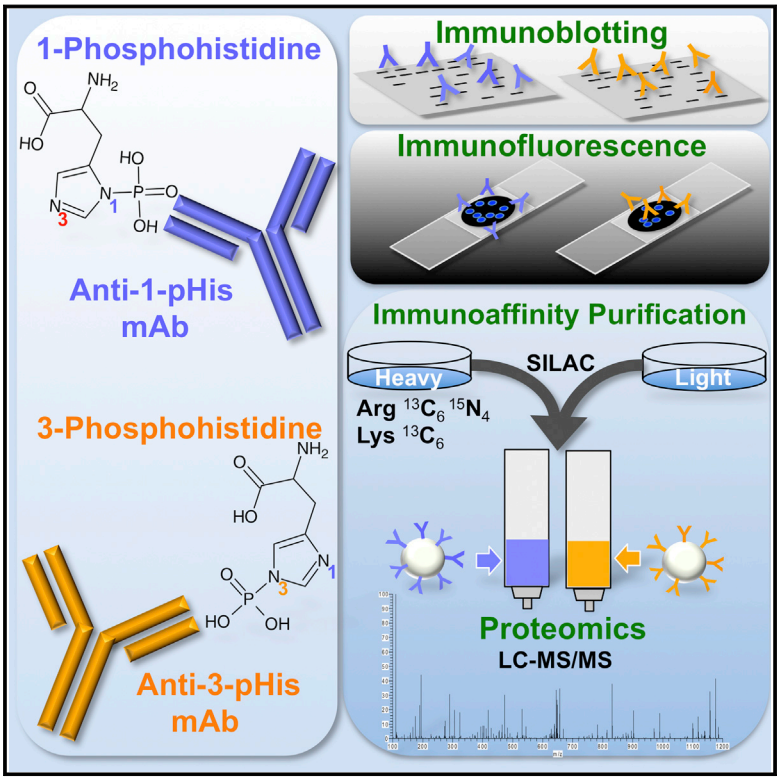

Highlights

- Sequence-independent monoclonal antibodies against phosphohistidine were developed
- pHis mAbs are isomer specific (1-pHis or 3-pHis) and do not bind pTyr
- pHis mAbs can be used in immunoblotting, IF, and immunoaffinity purification
- Immunofluorescence reveals roles for 1-pHis and 3-pHis in phagocytosis and mitosis

Authors

Stephen Rush Fuhs, Jill Meisenhelder, Aaron Aslanian, ..., Greg Lemke, John R. Yates III, Tony Hunter

Correspondence

hunter@salk.edu

In Brief

Sequence-independent monoclonal antibodies that specifically recognize histidine phosphorylation sites allow identification of pHis substrates and functional studies of this posttranslational modification, using a variety of immunological, proteomic, and biological assays.

Fuhs et al., 2015, Cell *162*, 198–210
July 2, 2015
http://dx.doi.org/10.1016/j.cell.2015.05.046

CellPress

Cell

Resource

Monoclonal 1- and 3-Phosphohistidine Antibodies: New Tools to Study Histidine Phosphorylation

Stephen Rush Fuhs,[1] Jill Meisenhelder,[1] Aaron Aslanian,[1,4] Li Ma,[1] Anna Zagorska,[2] Magda Stankova,[3] Alan Binnie,[3] Fahad Al-Obeidi,[3] Jacques Mauger,[3] Greg Lemke,[2] John R. Yates III,[4] and Tony Hunter[1,*]
[1]Molecular and Cell Biology Laboratory, Salk Institute for Biological Studies, La Jolla, CA 92037, USA
[2]Molecular Neurobiology Laboratory, Salk Institute for Biological Studies, La Jolla, CA 92037, USA
[3]Tucson Innovation Center, Sanofi, Tucson, AZ 85755, USA
[4]Department of Chemical Physiology, The Scripps Research Institute, La Jolla, CA 92037, USA
*Correspondence: hunter@salk.edu
http://dx.doi.org/10.1016/j.cell.2015.05.046

SUMMARY

Histidine phosphorylation (pHis) is well studied in bacteria; however, its role in mammalian signaling remains largely unexplored due to the lack of pHis-specific antibodies and the lability of the phosphoramidate (P-N) bond. Both imidazole nitrogens can be phosphorylated, forming 1-phosphohistidine (1-pHis) or 3-phosphohistidine (3-pHis). We have developed monoclonal antibodies (mAbs) that specifically recognize 1-pHis or 3-pHis; they do not cross-react with phosphotyrosine or the other pHis isomer. Assays based on the isomer-specific autophosphorylation of NME1 and phosphoglycerate mutase were used with immunoblotting and sequencing IgG variable domains to screen, select, and characterize anti-1-pHis and anti-3-pHis mAbs. Their sequence independence was determined by blotting synthetic peptide arrays, and they have been tested for immunofluorescence staining and immunoaffinity purification, leading to putative identification of pHis-containing proteins. These reagents should be broadly useful for identification of pHis substrates and functional study of pHis using a variety of immunological, proteomic, and biological assays.

INTRODUCTION

The majority of intracellular proteins are phosphorylated at any given time, and, while 9 of the 20 amino acids can be phosphorylated, the current focus has been on serine (Ser), threonine (Thr), and tyrosine (Tyr) phosphorylation, despite histidine phosphorylation (pHis) having been first identified over 50 years ago (Boyer et al., 1962). Ser, Thr, and Tyr all form acid-stable phosphoester (P-O) bonds upon phosphorylation (Attwood et al., 2007), whereas His forms heat and acid-labile phosphoramidate (P-N) bonds. Phospho-specific antibodies have enabled routine study of phosphoester protein phosphorylation, and the use of MS-based phosphoproteomics has identified thousands of phosphorylation sites in human cells, tissues, and tumors. The lack of specific antibodies with which to study pHis, and the relative instability of the P-N bond under typical conditions used for proteomics, have made it impossible to determine the prevalence of pHis. Early estimates suggest that pHis could be as abundant as pTyr (Matthews, 1995; Pesis et al., 1988), which comprises ~1% of all known phosphorylation in cells (Hunter and Sefton, 1980; Olsen et al., 2006). Since current biochemical and proteomic technologies have been optimized for preservation, enrichment, and detection of the phosphoester amino acids, pHis has remained largely invisible, and its importance has likely been underestimated.

A large family of His kinases and downstream signaling proteins, known as two-component regulatory systems, are widely employed by bacteria to link extracellular signals with transcription and chemotaxis. Similar phosphotransfer cascades function in plants to regulate processes such as ripening and circadian rhythms (Matthews, 1995). Its importance in these systems notwithstanding, whether or not pHis plays an important role in vertebrate cell signaling remains unresolved. NME1 and NME2 are the only mammalian protein-His kinases reported to date (Cai et al., 2014; Hartsough et al., 2002; Wagner and Vu, 1995), and there is growing evidence implicating these two closely related proteins in cancer and tumor metastasis (Thakur et al., 2011; Tso et al., 2013). Indeed, NME1 (aka Nm23-H1 or nucleoside diphosphate kinase, NDPK) was the first candidate metastasis suppressor gene identified (Steeg et al., 1988). NME family members are involved in intracellular nucleotide triphosphate homeostasis and in both physiological and pathophysiological cellular processes, such as proliferation, differentiation, development, apoptosis, cytokinesis, and dynamin-mediated endocytosis (Boissan et al., 2014; Conery et al., 2010). pHis is unique among phosphoamino acids in that two biologically relevant isomers occur. Both imidazole nitrogen atoms (N1 and N3) can be phosphorylated to generate 1-phosphohistidine (1-pHis) or 3-phosphohistidine (3-pHis) (Figure 1A). NME family members catalyze the transfer of phosphate from ATP onto NDPs through a 1-pHis enzyme intermediate. 3-pHis is used by bacterial His kinases to initiate phosphotransfer cascades and plays a role as an enzyme intermediate for phospholipase D and for several metabolic enzymes, including phosphoglycerate mutase (PGAM), succinyl-CoA synthetase (SCS), and ATP-citrate lyase (ACLY)(Kee and Muir, 2012). pHis regulatory sites have also been identified in a number of proteins with non-enzymatic

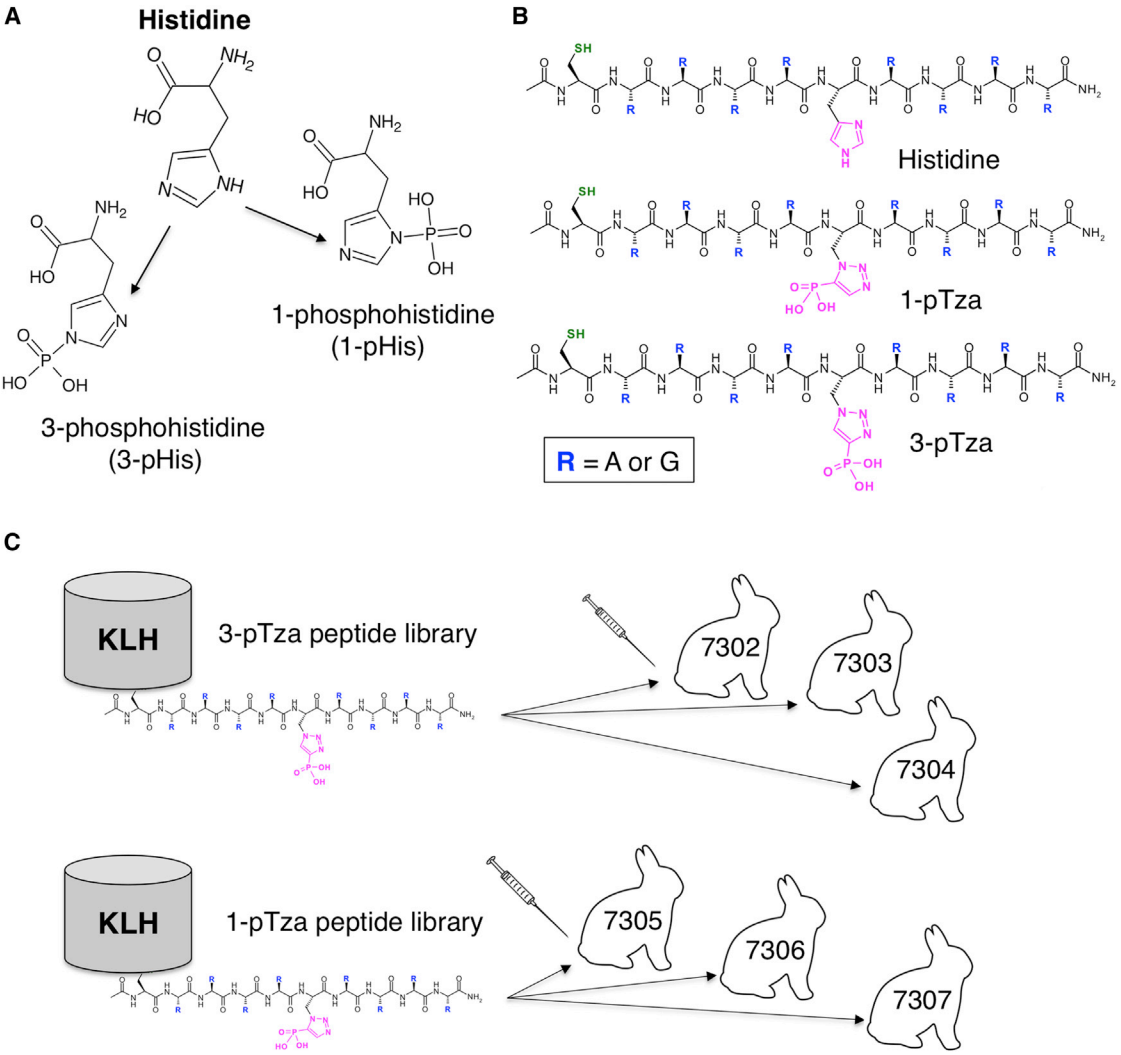

Figure 1. Incorporation of Non-hydrolyzable Phosphohistidine Analogs into Degenerate Peptide Libraries for Use as Immunogens

(A) Structure of histidine and the two pHis isomers: 1-phosphohistidine (1-pHis) and 3-phosphohistidine (3-pHis).

(B) Structures of the three synthetic peptide libraries used in this study in which either His or a stable pHis mimetic (1-pTza or 3-pTza) is flanked by randomized, neutral amino acids (alanine [A] and glycine [G]). Each library is composed of $2^8 = 256$ unique peptides (Figures S1A and S1B), acetylated at the N terminus and containing L-cysteine (Cys) for chemical ligation to KLH (Ac-Cys.G/A.G/A.G/A.G/A.***X***.G/A.G/A.G/A.G/A.G/A-CONH2).

(C) The peptide libraries were conjugated to the carrier protein keyhole limpet hemocyanin (KLH). Three rabbits were immunized with the 3-pTza library (7302, 7303, and 7304), and three rabbits were immunized with the 1-pTza library (7305, 7306, and 7307).

See also Figure S1.

functions. For example, phosphorylation of KCa3.1 (His358) and TRPV5 (His711) by NME2 promotes channel activation that is negatively regulated by a pHis-specific phosphatase (PHPT1) (Cai et al., 2014; Srivastava et al., 2006). Phosphorylation of GNB1 (His266) by NME2 activates Gs and regulates basal cAMP accumulation (Wieland et al., 2010). Histone H4 phosphorylation (His18) is highly conserved and was first observed in eukaryotes over 40 years ago (Besant and Attwood, 2012).

Recently, sequence-specific pHis polyclonal antibodies toward pHis18 in histone H4 have been generated (Kee et al., 2010). First- and second-generation "pan-pHis" polyclonal antibodies against 3-pHis have also been reported (Kee et al., 2013, 2015). However, these antibodies appear to be limited in their usefulness by their cross-reactivity with pTyr. Isoform-specific pHis monoclonal antibodies (mAbs) have not yet been developed. We used non-hydrolyzable phosphoryltriazolylalanine (pTza) pHis analogs (Kee et al., 2010; McAllister et al., 2011) incorporated into degenerate peptide libraries to immunize rabbits and develop selective anti-1-pHis and anti-3-pHis mAbs. We demonstrate that these mAbs do not cross-react with pTyr, appear to detect pHis in a sequence-independent manner, and can be used in a variety of immunological assays.

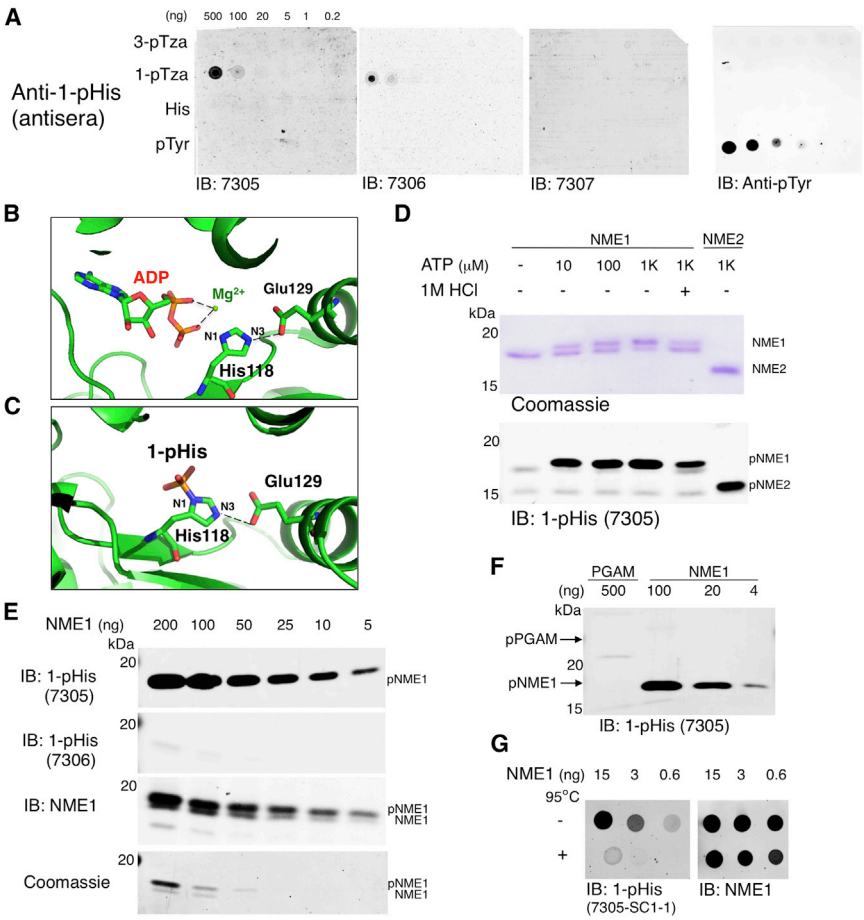

Figure 2. Screening of 1-pHis Antisera Using NME1 In Vitro Phosphorylation Assays

(A) Dot blot screening of 1-pHis antisera. The 1-pTza, 3-pTza, and His libraries (Figure 1B) were dissolved in water, and 1 μl of 1:5 serial dilutions were spotted directly on nitrocellulose and probed with antisera from rabbits 7305, 7306, and 7307. A synthetic pTyr peptide was included to control for pTyr cross-reactivity, and membranes were probed with pTyr mAb 4G10 as a positive control.

(B) Ribbon representation of PDB ID code 1NSP. NME1 was co-crystallized with ADP and Mg^{2+}, and the hydrogen bond between NME1 E129 with the N3 nitrogen on the catalytic H118 is shown as a dashed line.

(C) Phospho-NME1 (PDB ID code 4DY9) is shown to highlight that 1-pHis (but not 3-pHis) is formed on the catalytic His residue H118.

(D) NME1 and NME2 in vitro autophosphorylation assay. Recombinant NME1 and NME2 were incubated with up to 1 mM ATP at RT for 10 min. Negative controls were performed by omitting ATP or treating with 1 M HCl for 15 min at 37°C. Immunoblotting was performed with antiserum from rabbit 7305, and an identical gel was run in parallel and stained with Coomassie blue.

(E) 1-pHis detection limit assay. In-vitro-phosphorylated NME1 was diluted from 200 to 5 ng and blotted with 1-pHis antisera from rabbits 7305 and 7306, as well as NME1 antibodies. Identical gels were stained with Coomassie blue.

(F) 1-pHis isoform specificity. Recombinant PGAM (Figure 3E) and NME1 were autophosphorylated in vitro and blotted with 1-pHis antisera (rabbit 7305).

(G) Phospho-NME1 spot blots. In vitro phosphorylation of NME1 was performed as in Figures 2D and 2E, except reactions were stopped with the addition of 2% SDS (rather than sample buffer), treated with or without heating to 95°C for 10 min, diluted 1:5, and spotted directly on nitrocellulose. Representative immunoblots with mAb SC1-1 and NME1 antibodies are shown.

See also Figures S1 and S2.

RESULTS

Design of pHis mAb Immunogens: Incorporation of Non-hydrolyzable pHis Analogs into Degenerate Peptide Libraries

Previous attempts to make pHis antibodies using pHis itself as the antigen have been unsuccessful, presumably because the labile phosphoramidate bond is hydrolyzed too rapidly after immunization to elicit an immune response. The development of non-hydrolyzable phosphonate analogs of both isomers (1-phosphoryl-triazolylalanine [1-pTza] and 3-phosphoryl-triazolylalanine [3-pTza]) allowed us to develop a strategy for generating both 1-pHis- and 3-pHis-specific mAbs. We synthesized two peptide libraries consisting of 1-pTza or 3-pTza flanked by randomized sets of alanine (Ala) and glycine (Gly) to serve as immunogens. An unphosphorylated version with His in place of pTza was also synthesized (Figure 1B). MS analysis of the peptide libraries confirmed that the random incorporation of Ala and Gly matched the expected distribution of peptides sharing the same composition of 0–8 Ala and/or Gly residues (Figures S1A and S1B). The N-terminal Cys was used to couple the pTza libraries to KLH (keyhole limpet hemocyanin), and three rabbits were immunized for each pHis isomer (Figure 1C).

Development of Phospho-NME1 Screening Assay Demonstrates 1-pHis Antibody Specificity

Bleeds from immunized rabbits (7305, 7306, and 7307) were screened by dot blot using the 1-pTza library. To define pHis isoform specificity and control for cross-reactivity, the 3-pTza peptide library, a His control library, and a pTyr peptide (Nck pY105) were also included (Figure 2A). Antisera from two rabbits (7305 and 7306) detected only the 1-pTza immunizing library and did not cross-react with pTyr. While the synthetic pTza immunogen peptides were useful for preliminary antisera screening, protein samples with pure 1-pHis or 3-pHis were needed for screening antibodies for isomer specificity. Two in vitro phosphorylation assays capable of rapidly generating either pure 1-pHis or 3-pHis on proteins were developed using NME1/NME2 and PGAM, respectively. To generate 1-pHis, we utilized the unique properties of NME1/2, which autophosphorylate on a conserved catalytic His (H118) when incubated with ATP and Mg^{2+}. This occurs solely at the N1 position due to a conserved Glu (E129) that

H bonds with the protonated N3 nitrogen, leaving N1 able to accept the γ-phosphate from ATP (PDB ID codes 1NSP and 4DY9; Figures 2B and 2C) (Moréra et al., 1994). Autophosphorylation of recombinant NME1/2 occurred in an ATP dose-dependent fashion up to 1 mM ATP (Figure 2D). Reactions were stopped by addition of 5× sample buffer (pH 8.8) and immediately analyzed by a modified SDS-PAGE method without heating (Supplemental Experimental Procedures). Autophosphorylation on H118 was confirmed by liquid chromatography-tandem mass spectrometry (LC-MS/MS) with modifications to preserve and detect pHis (Figure S1C; Supplemental Experimental Procedures). Analysis by immunoblotting and Coomassie staining revealed a phosphorylation-dependent doublet (for NME1 though not NME2) with the slower migrating band representing phospho-NME1 (pNME1). 1 M HCl acid treatment at 37°C or omission of ATP reduced or abolished phosphorylation of NME1 (Figure 2D). Mutagenesis of the catalytic residue H118 prevented phosphorylation of NME1/2 (data not shown).

In-vitro-phosphorylated NME1 was used to measure the sensitivity of 1-pHis antisera (Figure 2E) and gauge titer as rabbits were boosted with antigen until titers peaked and stabilized. Identical samples were blotted with NME1 antibodies or stained by Coomassie as a loading control. Interestingly, 1-pHis was detected by rabbit 7305 antisera, but not by 7306 (Figure 2E), despite both binding 1-pTza peptides (Figure 2A). We also confirmed that 1-pHis antisera did not cross-react with 3-pHis. In-vitro-phosphorylated PGAM (pPGAM) was analyzed alongside 5- to 125-fold less NME1 (Figure 2F), and no 3-pHis signal was observed. Identical samples blotted with 3-pHis antisera (Figure 3F) served as a positive control for pPGAM detection. A method for rapid analysis of pHis was also developed for screening. pNME1 or pPGAM were directly spotted onto nitrocellulose to avoid potential loss of signal that may occur during SDS-PAGE. This allowed for comparison of mAb sensitivity by spotting limiting dilutions of the phosphoproteins. 1-pHis mAb SC1-1 was able to detect less than 600 pg of pNME1, and the signal was abolished when samples were heated at 95°C for 10 min to induce dephosphorylation, whereas NME1 detection was unaffected (Figure 2G).

Development of Phospho-PGAM Screening Assay Demonstrates 3-pHis Antibody Specificity

Bleeds from 3-pTza-immunized rabbits (7302, 7303, and 7304) were screened by dot blot (as described for 1-pTza antisera; Figure 2A), and only the 3-pTza immunizing library was detected (Figure 3A). PGAM is a glycolytic enzyme that converts 3-phosphoglycerate to 2-phosphoglycerate through a 3-pHis phosphoenzyme intermediate (Vander Heiden et al., 2010). Available crystal structures of pPGAM and PGAM co-crystallized with its phosphate donor (2,3-diphosphoglycerate [2,3-DPG]) show that only N3 of H11 is positioned to accept the phosphate from 2,3-DPG (PDB ID codes 1E58 and 2H4z; Figures 3B and 3C). To determine if PGAM could be phosphorylated in vitro, glutathione S-transferase (GST)-PGAM was incubated with 2,3-DPG (1 μM to 1 mM) (Figure 3D). Identical samples were heated at 95°C for 10 min, and immunoblotting with 3-pHis antisera revealed a heat-sensitive, 45 kDa band that was absent when 2,3-DPG was omitted. PGAM was subsequently cloned into a bacterial expression vector that allowed cleavage of the GST for analysis of untagged protein. PGAM was purified from *Escherichia coli* and incubated with or without 2,3-DPG. Autophosphorylation on H11 was confirmed by LC-MS/MS (Figure S1D), and immunoblotting with 3-pHis antisera revealed a heat-sensitive band at 25 kDa (Figure 3E) that was abolished by mutagenesis of H11 (data not shown).

To confirm that 3-pHis antisera did not cross-react with 1-pHis, pNME1 was analyzed alongside pPGAM, and no 1-pHis signal was detected (Figure 3F). As we observed for 1-pHis antisera, not all 3-pHis antisera that recognized the pTza analogs could bind pHis. Antisera from rabbits 7303 and 7304 (Figure 3F), but not from 7302, detected pPGAM. For this reason, we used splenocytes from rabbits 7303 and 7304 to generate hybridomas expressing 3-pHis mAbs in collaboration with Epitomics. To determine 3-pHis mAb sensitivity, in-vitro-phosphorylated PGAM was spotted directly on nitrocellulose. A representative immunoblot with 3-pHis mAb SC39-4 showed phospho-PGAM was detected down to ~10 ng in a heat-sensitive manner (Figure 3G).

Screening and Sequencing of 1-pHis mAb Hybridomas Yielded Three Unique Sequence-Independent mAbs

Splenocytes from rabbit 7305 were used for generation of 1-pHis hybridomas, as described for 3-pHis hybridomas. Several thousand hybridoma cell lines generated from rabbit 7305 were initially screened by ELISA in 96-well plates coated with the immunizing 1-pTza peptide library (data not shown). 48 ELISA-positive multiclonal cell lines were selected for secondary screening using several assays, including the pNME1 assays described above. Since pHis is known to be involved in bacterial two-component signaling, we also developed a bacterial-based screening assay in which *E. coli* transformed with a pGEX-NME1 plasmid were induced with isopropyl β-D-1-thiogalactopyranoside (IPTG) for 3 hr to overexpress the 1-pHis-positive control protein GST-NME1. Crude lysates were loaded on preparative minigels (i.e., a single sample well) and transferred to polyvinylidene fluoride (PVDF) membranes, which were clamped into a slot blotting apparatus (Supplemental Experimental Procedures). Membranes were probed with cell supernatants from the 48 ELISA-positive multiclonal lines (Figure S2A). The top three multiclonal cell cultures (MC1, MC50, and MC77) were selected for subcloning based on multiple assays (ELISA, immunoblotting, peptide dot blots, etc.). Similar assays were used to screen subclones for the final selection of 1-pHis mAb hybridoma cell lines. For example, small-scale screens were performed using *E. coli* lysates treated with or without heat (Figure S2B). Identical membranes were probed with crude 1-pHis antisera, and the 1-pHis mAbs exhibited significantly decreased background. Since GST-NME1 is highly overexpressed in these cells, it is not surprising that it was the strongest signal detected; however, many other heat-sensitive bands were also detected (Figure S2B). Next, we sought to determine the extent to which these mAbs could detect 1-pHis in mammalian cells, by performing a similar screen using lysates from a stably transfected FLAG-NME1 293 cell line (Figure S2C). Membranes were probed simultaneously with FLAG-M2 and 1-pHis mAbs (Figure S2D). Multiple heat-sensitive

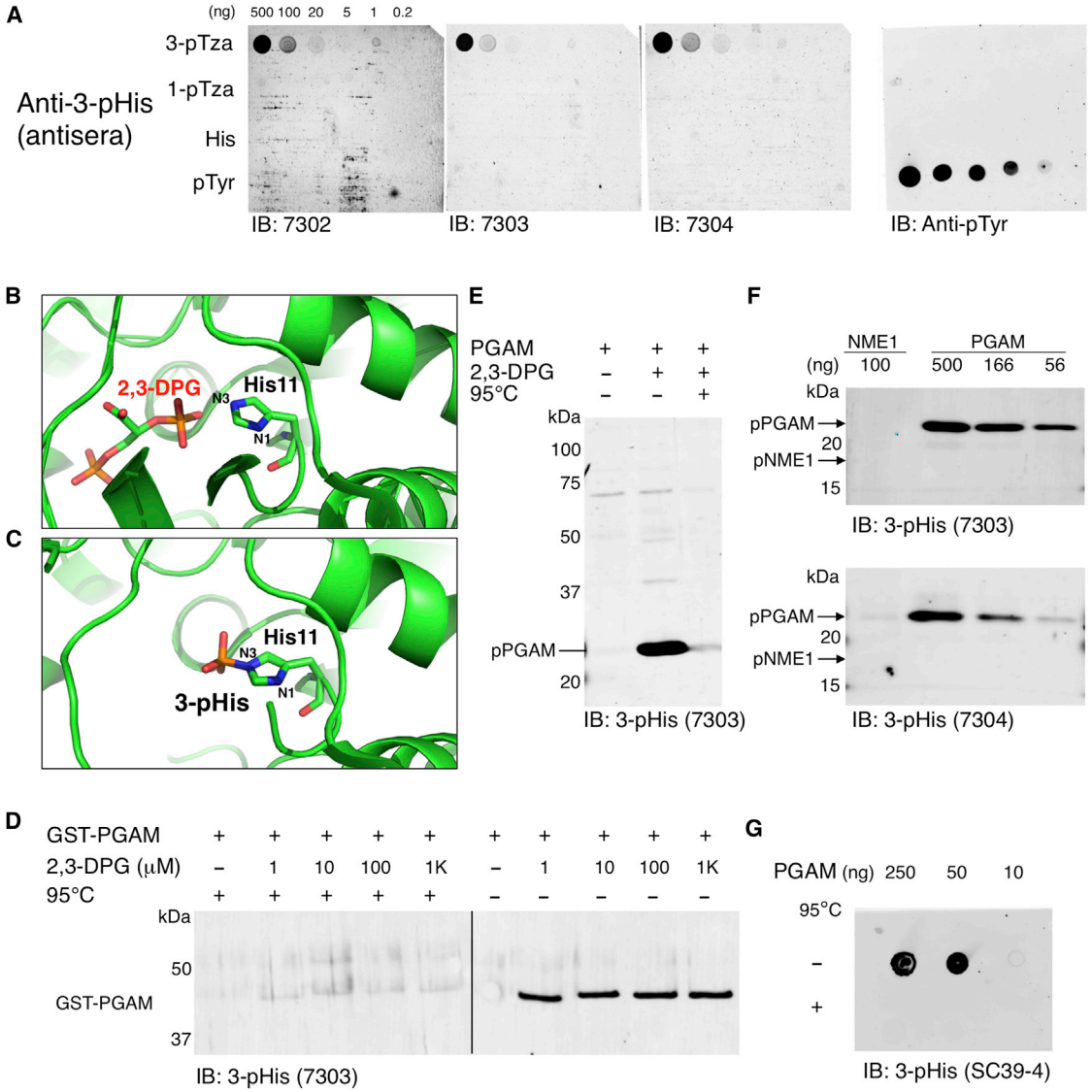

Figure 3. Screening of 3-pHis Antisera by PGAM In Vitro Phosphorylation Assays

(A) Dot blot screening of 3-pHis antisera from rabbits 7302, 7303, and 7304 was performed as described in Figure 2A.

(B) Ribbon representation of PDB ID code 4HZE shows the relative positions of N1 and N3 in H11 of PGAM and its phosphate donor 2,3-DPG.

(C) Structure of PGAM (PDB ID code 1E58) highlighting 3-pHis formation on the catalytic His residue H11.

(D) GST-PGAM fusion protein was autophosphorylated in vitro by addition of increasing concentrations of 2,3-DPG. Reactions were stopped by the addition of 5× sample buffer (pH 8.8) and treated with or without heating to 95°C for 10 min.

(E) Purified PGAM was autophosphorylated in vitro by incubation with 2,3-DPG for 10 min at 30°C. Reactions were stopped by addition of 5× sample buffer (pH 8.8) and treated with or without heat.

(F) 3-pHis isoform specificity. Recombinant NME1 and PGAM were autophosphorylated in vitro by incubation with ATP or 2,3-DPG, respectively, and blotted with 3-pHis antisera from rabbits 7303 and 7304.

(G) Phospho-PGAM spot blots. In vitro phosphorylation of PGAM was performed as in Figure 3E, except reactions were stopped by the addition of 2% SDS. Reactions were treated with or without heat, diluted 1:5, and spotted directly on nitrocellulose. A representative immunoblot with 3-pHis mAb SC39-4 is shown. See also Figures S1 and S2.

bands were detected, further suggesting that 1-pHis mAbs are able to detect 1-pHis regardless of sequence context. Sequencing of the immunoglobulin G (IgG)-variable domains (V_H and V_L) revealed that three unique sequences were encoded by subclones SC1-1, SC50-3, and SC77-11.

Screening and Sequencing of 3-pHis mAb Hybridomas Yielded Three Unique Sequence-Independent mAbs and One Sequence-Dependent mAb

Hybridomas generated from combined splenocytes from rabbits 7303 and 7304 were screened by ELISA using the 3-pTza

peptide library (data not shown). 30 ELISA-positive multiclonal cell lines were selected for secondary screening using 3-pHis-specific assays, including pPGAM as described above. The four best 3-pHis mAb cell lines (MC39, MC44, MC56, and MC60) were subcloned, resulting in up to 12 ELISA-positive subclones from each parental multiclone. *E. coli* transformed with a pGEX-PGAM plasmid were induced, and crude lysates were supplemented with 2,3-DPG, spiked with purified, untagged PGAM, and loaded on preparative minigels. High-throughput, slot blotting was performed as described for 1-pHis mAb hybridomas (Figure S2E).

A small-scale screen was performed in parallel using identical *E. coli* lysates treated with and without heat (Figure S2F). All of the detected bands were heat sensitive, indicating the mAbs are 3-pHis-specific. Strong signals for the positive control proteins, GST-PGAM and PGAM (untagged), as well as many other heat-sensitive bands, were detected by SC39s, SC56s, and SC60s, suggesting that these mAbs lack strong sequence specificity but do not produce an identical pattern of bands. In contrast, SC44s primarily detected a strong band corresponding to bacterial SCS (Figures S2E and S2F). SCS also uses a 3-pHis phosphoenzyme intermediate (Fraser et al., 2000), and SC44s detected both bacterial SCS and mammalian SCS and ACLY (Figure S2G), which share the sequence motif G-**H**-A-G-A (Figure S2H). Cell lysates prepared from a stably transfected HEK293 cell line expressing FLAG-NME1 were blotted with 3-pHis mAb SC39-4, and 3-pHis on endogenous pPGAM was detected, but not 1-pHis on FLAG-NME1, indicating the 3-pHis mAbs do not cross-react with 1-pHis generated in vivo (Figure S2I). Sequence analysis of 3-pHis mAb V_H and V_L domains allowed us to identify SC39-4, SC56-2, and SC60-2 as unique, sequence-independent 3-pHis mAbs, as well as a distinct sequence-dependent mAb SC44-8 that has bias toward the A/G motif present in SCS and ACLY.

1-pHis and 3-pHis Antibodies Detect Various pTza Peptides of Defined Sequence

Synthetic 1-pTza and 3-pTza peptide dot blot arrays were used to confirm the pHis isoform specificity of the pHis mAbs and determine if they have any local amino acid sequence specificity. We synthesized peptides of a defined sequence based on the best-characterized mammalian pHis proteins: ACLY, NME1, PGAM, histone H4, KCa3.1, and GNB1. Peptides corresponding to the pHis sites in these proteins were synthesized with His, 1-pTza, or 3-pTza, flanked by four amino acids on either side (Figure S3; Table S2). Serial dilutions of each defined-sequence peptide, the immunizing pTza, and the control His peptide libraries were spotted onto nitrocellulose and blotted with affinity-purified, polyclonal 1-pHis, or 3-pHis antibodies. The 3-pHis antibodies bound only the 3-pTza peptides, and the 1-pHis antibodies bound only the 1-pTza peptides, regardless of sequence (Figure 4A). Identical membranes were probed with 1-pHis mAbs as part of our screening process to select mAbs with the broadest sequence recognition (Figure 4B). The 1-pHis mAbs displayed similar binding profiles and detected as little as 1 ng of the NME1/2 H118 peptide. Each of the 1-pTza peptides tested was detected, suggesting these mAbs will be useful for detecting 1-pHis in a broad range of sequence contexts. Since 3-pHis mAbs did not cross-react with either 1-pTza or His peptides (Figure 4A), we probed peptide arrays consisting of just 3-pTza peptides, including a PGAM peptide, to determine their sequence specificity (Figure 4C). In contrast to the 1-pHis mAbs, the 3-His mAbs displayed some variation in binding profiles. 3-pHis mAb SC39-4 was able to detect all 3-pTza peptides down to 800 pg; however, binding to the KCa3.1 peptide was relatively poor (100 ng). 3-pHis mAb SC56-2 showed similar binding characteristics; however, it was better at detecting the KCa3.1 peptide (4 ng), while being worse at binding the GNB1 peptide. SC44 detected the A/G motif peptide (based on ACLY) and the immunizing peptide library down to 160 and 800 pg, respectively, confirming its sequence bias.

pHis mAbs Do Not Cross-React with pTyr Peptides

Since some of the first described pTyr mAbs cross-reacted with pHis (Frackelton et al., 1983), and recently reported polyclonal pHis antibodies displayed only a 10-fold higher selectivity for pHis over pTyr (Kee et al., 2013), we tested our pHis mAbs for cross-reactivity using synthetic pTyr peptides. Serial dilutions of pTyr peptides (Nck and the Eck/EphA2 and FAK tyrosine kinases) were spotted on nitrocellulose along with their unphosphorylated counterparts. The pTyr mAb 4G10 detected only the pTyr peptides (Figure 4D), whereas none of the peptides were detected by 3-pHis (Figure 4E) or 1-pHis mAbs (Figure 4F).

pHis mAbs Do Not Cross-React with pTyr Proteins in Cell Lysates

To test for pTyr cross-reactivity of our pHis mAbs on cell lysates, cultures of v-Src-transformed NIH/3T3 fibroblasts (p*src*11; Johnson et al., 1985) were pre-incubated with 1 mM orthovanadate for 30 min to enhance pTyr signals. Non-transformed fibroblasts (pancreatic stellate cells PaSC) were tested in parallel as a negative control. To preserve pHis in cell lysates for analysis by immunoblotting, we adopted a modified SDS-PAGE method to maintain the sample pH above 8 to stabilize pHis (Supplemental Experimental Procedures). As expected, pTyr mAb 4G10 detected an elevated signal in the p*src*11 cells, but not in the PaSC-negative control cells, but neither the 1-pHis nor 3-pHis mAbs detected the elevated pTyr signal in p*src*11 cells (Figure 5A).

pHis mAbs Detect pHis Proteins in Mammalian Cell Lysates

A number of heat-sensitive bands were detected in the p*src*11 and PaSC lysates by 1- and 3-pHis mAbs. Next, we immunoblotted lysates from a variety of other mammalian cell lines to characterize the pHis levels in different cell types. 3-pHis mAbs SC39-4 (Figure 5B) and SC44-8 (Figure 5C) were used to blot lysates from 293 cells, and 1-pHis mAb SC1-1 was used to blot lysates from several pancreatic cancer (PC) cell lines and HPDE6, a normal pancreatic epithelial cell line (Figure 5D). Common patterns of heat-sensitive bands were observed, indicating many proteins in these cancer cell lines are similarly regulated by 1-pHis modification. Lysates from FLAG-NME1 293, HeLa, C2C12, and NME1- and NME2-overexpressing (OE) melanoma cell lines (Hamby et al., 2000) were also blotted with 1-pHis mAb SC1-1 (Figure 5E). 1-pHis was

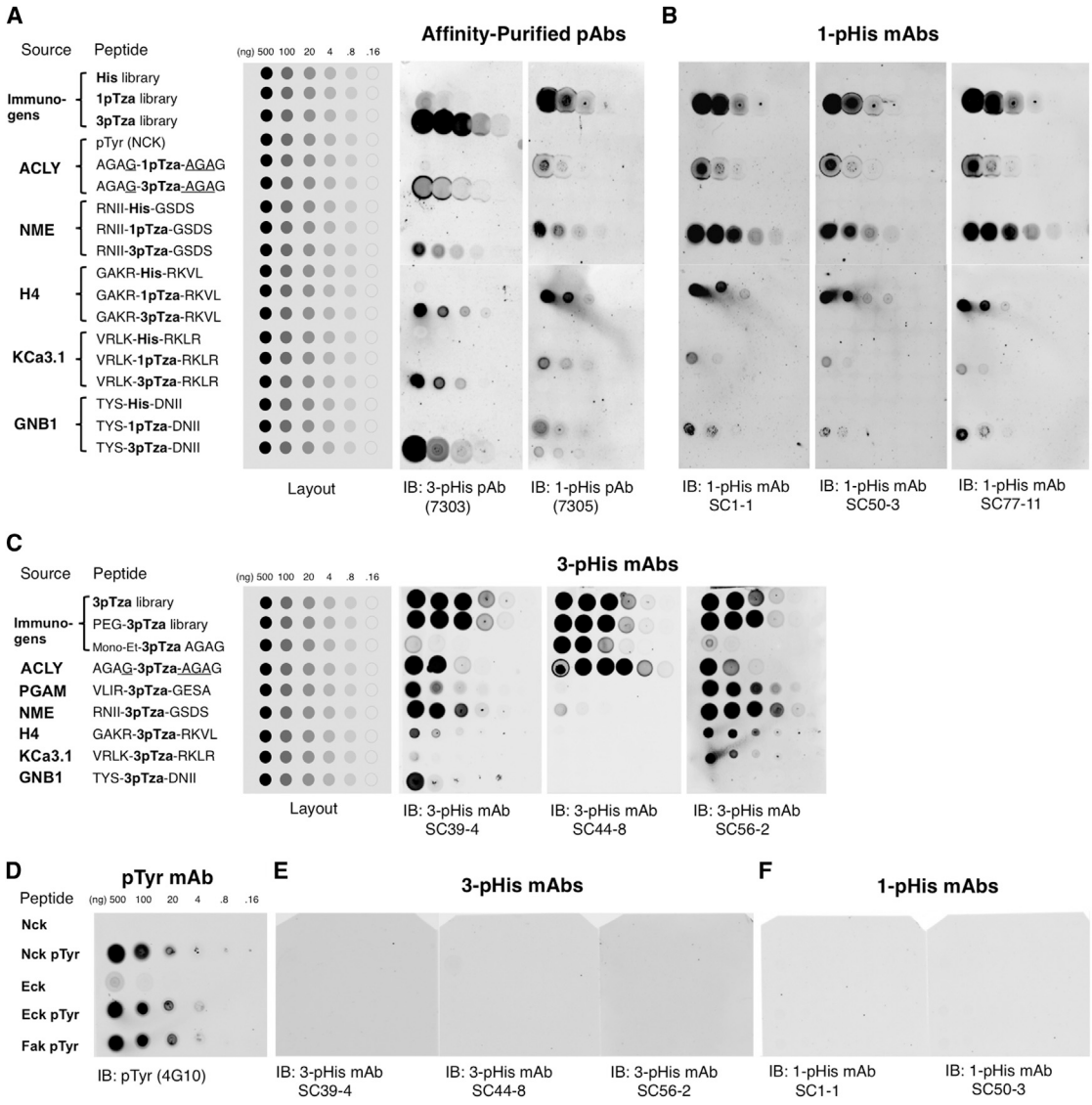

Figure 4. 1-pHis and 3-pHis mAbs Detect Isomer-Specific pTza Peptides, but Not pTyr

(A and B) Synthetic peptide dot blot arrays consisting of the His, 1-pTza, or 3pTza libraries (Figure 1B) and a pTyr (NCK) peptide, and peptides with His, 1-pTza, or 3pTza incorporated into defined sequences (based on the pHis protein substrates: ACLY, NME1/2, histone H4, KCa3.1, and GNB1) were spotted on nitrocellulose and probed with (A) affinity-purified polyclonal 3-pHis (7303) or 1-pHis (7305) antibodies or (B) 1-pHis mAbs SC1-1, SC50-3, and SC77-11.

(C) 3-pTza peptide dot blot characterization of 3-pHis mAbs. A partially deprotected, mono-ethyl ester version of the ACLY-based peptide (AGAG-mono-Et-3-pTza-AGAG) was also included. (A–C) The layout of spotted peptide dilutions (500–0.16 ng) are shown in gray boxes. The peptide sequences and their sources are indicated to the left of the peptide layouts.

(D–F) Synthetic pTyr peptide dot blots. Peptides based on Nck, Eck, and FAK were spotted on nitrocellulose and probed with (D) pTyr mAb 4G10, (E) 3-pHis mAbs SC39-4, SC44-8, and SC56-2, or (F) 1-pHis mAbs SC1-1 and SC50-3.

See also Figure S3.

detected on NME family members in mouse, human, and bacterial cells, including NME1, NME2, NME4, NME5 (Figures S4A–S4C), and NME7 (data not shown), despite differing sequences flanking the pHis residue (Figure S4A), as well as the *E. coli* NME1 homolog NDK (Figure S4C). While the major pHis proteins detected appear to be known enzymes (i.e., NME1/2 [1-pHis], PGAM, SCS, and ACLY [3-pHis]), the detection of many unidentified, heat-sensitive bands, particularly by the 3-pHis mAbs, suggests they will be useful in identifying many pHis substrates.

Immunofluorescence Staining Reveals Association of 1-pHis with the Outer Membrane of Phagosomes

To test the ability of these mAbs to detect pHis proteins by immunofluorescence staining, HeLa cells were stained with the 1-pHis mAb SC1-1. We observed a distinct staining pattern in

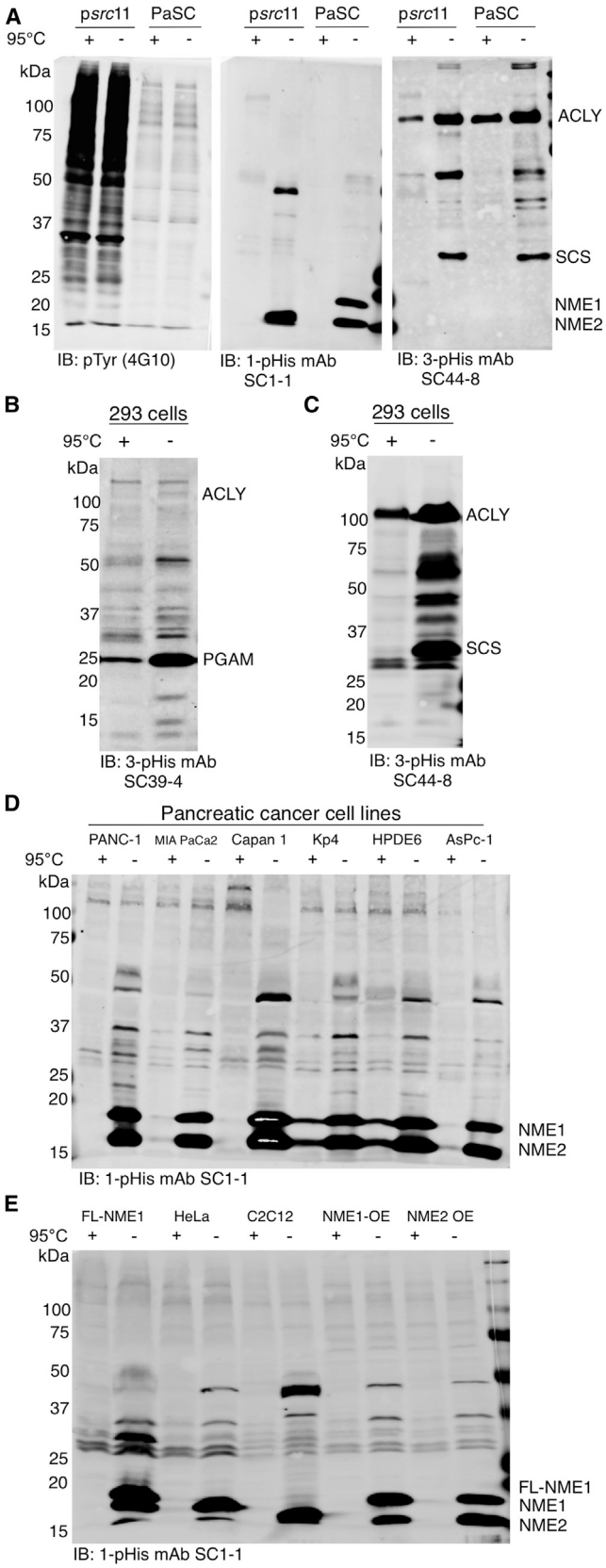

Figure 5. pHis, but Not pTyr, Proteins Are Detected in Mammalian Cells

(A) Src-transformed and non-transformed fibroblast cell lines (psrc11) and pancreatic stellate cells (PaSCs) were analyzed by immunoblotting with pTyr, 1-pHis, or 3-pHis mAbs. Cells were pre-treated with 1 mM sodium orthovanadate for 30 min prior to lysis.

(B and C) HEK293 cell lysates were immunoblotted with 3-pHis mAbs SC39-4 and SC44-8.

(D and E) Pancreatic cancer cell lysates, FLAG-NME1 293, HeLa, C2C12, and NME1- or NME2-overexpressing (OE) melanoma cells were immunoblotted with 1-pHis mAb SC1-1. All lysates (A–E) were prepared by scraping cells into 2× sample buffer (pH 8.8) and treated with or without heating for 10 min.

See also Figure S4.

which most cells had a large (1–2 μm) compartment that stained strongly in the surrounding region but lacked interior pHis staining (Figure 6A). We surmised that these might be acidic compartments, such as phagosomes or autophagosomes, and proceeded to test this hypothesis by using primary murine macrophages to look for specific staining of phagosomes. Macrophages isolated from bone marrow were incubated with fluorescently labeled dextrans to track internalization into phagosomes. Cells were also incubated with LysoTracker prior to fixation to label acidic compartments. 1-pHis staining was absent in nuclei, as well as the interior of phagosomes in macrophages co-labeled with the internalized dextrans and LysoTracker, but staining was pronounced in the regions surrounding these compartments (Figures 6B–6D). Remodeling of the actin cytoskeleton supports the extension of pseudopodia at sites of particle engulfment and F-actin assembles around nascent phagosomes. Co-staining with mAb SC1-1 and phalloidin-TRITC revealed a lack of co-localization of 1-pHis with actin filaments (Figure 6E).

3-pHis mAb Immunofluorescence Reveals Staining of Centrosomes, Spindle Poles, and Midbodies

Macrophages stained with 3-pHis mAbs displayed a pattern distinct from 1-pHis staining. Punctate structures were observed throughout the cytosol; however, no co-localization was observed when antibodies specific for organelle markers (e.g., ATP synthase, LC3, Rab5, α-tubulin, and LAMP1; Figures S5A–S5B; data not shown) were tested for co-staining. In contrast to macrophages, staining of HeLa cells with 3-pHis mAbs was primarily nuclear (though curiously absent from nucleoli), and distinctive cell-cycle-dependent patterns were observed. Prometaphase cells through telophase cells displayed remarkable 3-pHis staining of spindle poles (Figures 6F–6K). Interphase cells displayed staining of centrosomes, and cells in prophase were observed with duplicated centrosomes (Figure 6G). An apparent burst of 3-pHis signals was observed in dividing cells, and this seemed to last from prometaphase through anaphase. To confirm this observation, HeLa cells were co-stained with 3-pHis mAbs and spindle pole markers Aurora-A and γ-tubulin (Figures 6H and 6I). To demonstrate that 3-pHis mAbs stained primarily spindle poles, and not spindles, cells were co-stained with α-tubulin (Figure 6J). 3-pHis mAbs also stained structures devoid of Aurora-A, γ-tubulin, and α-tubulin in both HeLa and U2Os cells, and these appeared to be the midbody of cells in late telophase. (Figures 6H–6K and

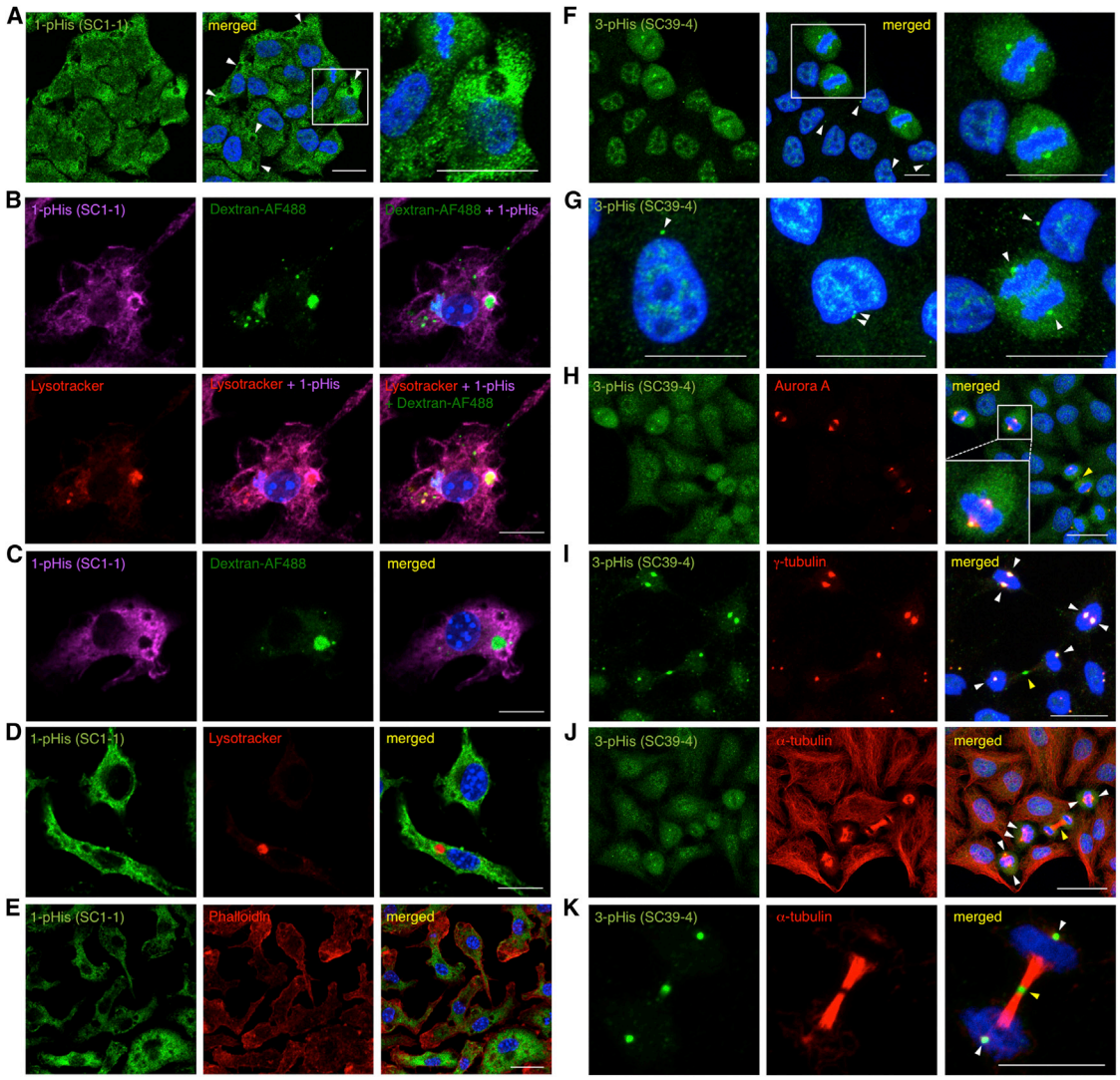

Figure 6. 1-pHis mAbs Negatively Stain Macrophage Phagosomes, and 3-pHis mAbs Stain Centrosomes and Spindle Poles in HeLa Cells

(A) HeLa cells were fixed with PFA and stained with 1-pHis mAb SC1-1. White arrows indicate acidic compartments.

(B) Macrophages were fed Dextran-AF488 and labeled with LysoTracker for 60 min prior to fixation with PFA, and staining with 1-pHis mAb SC1-1 was detected by Cy5-conjugated secondary antibodies. Scale bar, 10 μm.

(C) Macrophages were incubated with Dextran-AF488 for 60 min, and staining with mAb SC1-1 was detected by Cy5-conjugated secondary antibodies.

(D) Macrophages were labeled with LysoTracker for 60 min prior to fixation, and mAb SC1-1 staining was detected by AF-488-conjugated secondary antibodies.

(E) Co-staining of macrophages with mAb SC1-1 and Phalloidin-TRITC.

(F–K) HeLa cells were fixed with PFA (F and G) or pre-permeabilized with 0.5% Triton X-100 and fixed with PFA (I) and (K) or methanol (H) and (J) and stained with 3-pHis mAb SC39-4 alone (F and G) or co-stained with Aurora A (H), γ-tubulin (I), or α-tubulin (J and K) antibodies. (F) Metaphase cells are shown in an expanded view in the right panel. (G) From left to right, interphase, early prophase, and anaphase cells are shown. (H–K) Cells in metaphase, prometaphase, and telophase are shown. White arrows indicate centrosomes and spindle poles, and yellow arrows indicate midbodies in telophase cells. Nuclei were visualized with DAPI. Scale bar, 20 μm.

See also Figure S5.

S5C–S5E). A series of negative controls using the immunizing pTza peptide libraries were performed. Only the 1-pTza peptides could block 1-pHis staining (Figures S5F–S5I and S5P–S5Q), while only the 3-pTza peptides could block 3-pHis staining (Figures S5K–S5N and S5R–S5S). Additionally, boiling slides for 10 min in citrate buffer reduced both 1-pHis and 3-pHis staining (Figures S5J and S5O).

Enrichment and Identification of Proteins by pHis mAb Immunoaffinity Purification and SILAC LC-MS/MS

Traditional immunoprecipitation methods are not amenable to pHis preservation and detection. A method for immunoaffinity purification of pHis substrates using immobilized pHis mAbs was developed. Reusable pHis mAb resins were packed in chromatography columns and used to enrich pHis phosphoproteins

Table 1. SILAC Ratios Determined by LC-MS/MS Analysis Indicate Enrichment of Known pHis Proteins by pHis mAb Immunoaffinity Purification

Protein	Sequence	Site	1-pH E1	1-pH E2	3-pH E1	3-pH E2
NME1[a]	QVGRNIIHGSDSVES	H118	15.05	51.86	3.18	2.14
NME2[a]	QVGRNIIHGSDSVKS	H118	15.59	55.96	3.46	–
NME4	HISRNVIHASDSVEG	H151	–	–	–	–
NME5[b]	DDLRNALHGSNDFAA	H127	–	–	–	–
NME6[b]	TDTRNTTHGSDSVVS	H129	–	–	–	–
NME7	DGIRNAAHGPDSFAS	H206	–	–	–	–
Histone H4[a]	GKGGAKRHRKVLRDN	H18	19.14	9.8	22.82	17.9
KCa3.1[b]	FRQVRLKHRKLREQV	H358	–	–	–	–
TRPV5[b]	LRQNTLGHLNLGLNL	H711	–	–	–	–
GNB1[a]	QELMTYSHDNIICGI	H226	–	–	–	1.21
PGAM	YKLVLIRHGESAWNL	H11	–	4.25	4.01	2.44
ACLY	SSEVQFGHAGACANQ	H760	5.29	7.2	11.62	2.99
SCS	PPGRRMGHAGAIIAG	H299	–	1.68	–	–
P-Selectin[b]	GKCPLNPHSHLGTYG	H771	–	–	–	–
TUBB[a]	GNNWAKGHYTEGAEL	H105[c]	3.55	4.49	4.33	2.09
TCP1[a]	EETERSLHDAIMIVR	H346[c]	6.10	5.99	5.98	3.20
YWHAB[a]	KTALCFRHLMKQLLN	H202[c]	–	2.04	7.43	1.63
LDHA[a]	GEMMDLQHGSLFLRT	H67[c]	4.18	6.50	6.60	3.08
RPS3A	LGKLMELHGEGSSSG	H232[c]	7.21	9.10	10.41	4.98
GAPDH	TMEKAGAHLQGGAKR	H111[c]	3.40	4.45	4.76	3.32

Annotated pHis sites in protein sequences are underlined. SILAC ratio (light/heavy) indicates fold enrichment of proteins by pHis mAb affinity purification. Values from two sequential elution fractions (elution 1 [E1] and elution 2 [E2]) are reported as the median value of all quantified peptides that correspond to the listed protein. –, not detected. See also Figure S6 and Table S1.

[a]Related protein family members or isoform(s) were enriched.

[b]Not expressed in cell line tested.

[c]Sequences from pHis phosphopeptides detected by MS (Lapek et al., 2015).

from cell lysates prior to analysis by LC-MS/MS (Supplemental Experimental Procedures). pNME1 and pPGAM were used to test the pHis isomer selectivity of the high-density mAb columns. NME1 and PGAM were phosphorylated in vitro, denatured (6 M urea [pH 10]), mixed together, and incubated with either a 1-pHis or 3-pHis mAb column. Purification fractions were immunoblotted with 1- and 3-pHis mAbs, as well as NME1 and PGAM antibodies, and quantification demonstrates that pNME1 was enriched in elution fractions from the 1-pHis mAb column, while pPGAM was enriched in elutions from the 3-pHis mAb column (Figures S6A and S6B).

In order to determine which proteins bind the columns in a pHis-dependent manner and which are likely false positives that bind non-specifically, we used stable isotope labeling by amino acids in cell culture (SILAC) to metabolically label FLAG-NME1 293 cells. Initially, both the light- and heavy-labeled (Arg $^{13}C_6$ /$^{15}N_4$ and Lys $^{13}C_6$) cells were lysed using identical denaturing and alkaline conditions (6 M urea [pH 10]) to preserve pHis. The heavy lysates were then acidified (pH 6) and heated at 65°C for 30 min to reduce pHis. A dramatic decrease of pHis in the heavy lysates was confirmed by immunoblotting (data not shown). Both lysates were neutralized, diluted (1:5 to 1 M urea [pH 8]), and mixed together, and one half was passed over the 1-pHis mAb column, while the other half was passed over the 3-pHis mAb column. LC-MS/MS analysis was performed on tryptic peptides derived from proteins that eluted off the columns at pH 11. A SILAC ratio (light/heavy) was calculated for each peptide to determine which proteins were enriched in the untreated, light versus heavy lysates that had been treated to reduce pHis. We observed significant enrichment of NME1/2 (55-fold) by the 1-pHis mAb column, as well as enrichment of PGAM (4-fold) and the other known 3-pHis proteins, including histone H4 (22-fold) and ACLY (11-fold). Proteins corresponding to recently identified pHis phosphopeptides (Lapek et al., 2015), including TUBB, TCP1/CCT1, YWHAB, LDHA, RPS3A, and GAPDH were also enriched from 5- to 11-fold (Tables 1 and S1). In all, 630 proteins (58% of proteins quantified in 1-pHis column elutions E1–E3) and 506 proteins (54% of 3-pHis E1–E3) were enriched by at least 2-fold (Table S1) for a total of 786 different proteins. 280 of these were unique to the 1-pHis column, and 156 were unique to the 3-pHis column. Gene ontology analysis by biological processes (DAVID v.6.7; Huang et al., 2009) revealed that 97 of the 786 genes are involved in cell-cycle processes, including PP1, CDK1, cyclin B1, CUL1, and multiple proteasome subunits. Network analysis (STRING v.9.1; Franceschini et al., 2013) was performed to visualize the protein-protein interaction network of these cell-cycle-related genes (Figure S6C) with known pHis proteins (Table 1).

DISCUSSION

Our goal was to develop tools for the study of pHis in mammalian cells and to begin to determine its importance as a regulatory process in normal cells and in diseases, such as cancer. Our immunoblotting and proteomic data (Tables 1 and S1) suggest that these mAbs can recognize pHis independent of sequence context. However, little is known regarding the prevalence and relative levels of pHis proteins in mammalian cells, making it unclear whether all pHis substrates are recognized. For example, NME1/2 were the major cellular 1-pHis proteins detected by the 1-pHis mAbs, but this could reflect either a sequence bias of our 1-pHis mAbs (perhaps influenced by our screening approach) or that abundant expression levels of NME1/2 combined with their ability to autophosphorylate results in stronger detection by immunoblotting.

As is the case with pTyr blotting, activation of specific signaling pathways or enrichment of certain proteins by fractionation or immunoprecipitation prior to immunoblotting may be necessary to visualize low abundance, organelle-specific, or protein substrates with low stoichiometry of phosphorylation. The greater thermodynamic instability of 1-pHis versus 3-pHis may also contribute to difficulty in detecting some 1-pHis proteins. While detection of pNME1/2 by 1-pHis mAb immunoblotting is quite heat sensitive, brief heat treatment may not be harsh enough to reduce pHis in all proteins. There is a prominent, heat-resistant doublet detected in most of these cell lines (Figures 5D and 5E) that we suspect is NME4, the mitochondrial NME family member (Figure S4B).

Striking differences were observed between 1-pHis and 3-pHis mAb immunofluorescence staining. SC1-1 will be useful for studying acidic compartments (i.e., phagosomes, autophagosomes, and lysosomes) since staining is absent from the interior of these acidic compartments and often very bright in the surrounding regions. Analysis of the ''phagosome proteome'' identified NME2 as an outer membrane associated phagosomal protein (Garin et al., 2001). Dynamin-2 is required for macrophage phagocytosis (Gold et al., 1999), and NME1/2 were recently shown to interact with dynamin and dynamin-induced tubules and be required for efficient dynamin-mediated endocytosis by providing a localized source of GTP (Boissan et al., 2014). The strong 1-pHis signals we observed in regions surrounding phagosomes (Figures 6A–6E) could be the local, enzymatic activity of NME1/2 working to replenish GTP. Alternatively, the 1-pHis signals could reflect the presence of non-enzymatic, pHis protein substrates that are phosphorylated by NME1/2 or an unknown His kinase.

The 786 enriched proteins (Table S1) represent a starting point for identification and analysis of the mammalian pHis proteome. We preserved existing pHis on proteins in the lysates as fully as possible (i.e., denaturing and alkaline conditions to prevent protein phosphatase driven- or acid-catalyzed hydrolysis). However, we do not yet know which conditions or stimuli induce or increase pHis (analogous to epidermal growth factor or orthovanadate treatment for pTyr) to increase the yield of pHis proteins. As it stands, the most abundant proteins with the highest stoichiometry of His phosphorylation and stability are most likely to have been observed and quantified. Therefore, the complete list of pHis substrates is likely to be significantly longer than what we have detected. The enrichment of cell-cycle proteins by pHis mAbs is of great interest, since we also observe specific staining of mitotic structures by 3-pHis mAbs (i.e., spindle poles, centrosomes, and midbodies (Figures 6F–6K and S5C–S5E) that indicates pHis signals might be critical for regulating multiple cell-cycle events. The 97 cell-cycle-related proteins analyzed by STRING v.9.1 have multiple interaction nodes that fall into seven main categories: proteasome, cytokinesis, ribosome, cell-cycle regulation, protein phosphatase PP1, chromosome condensation, and chromatin and spindle organization (Figure S6C). In addition, gene ontology analysis (DAVID v.6.7) by biological processes revealed that 239 of the enriched proteins correspond to genes involved in nucleic acid-related processes, including (in order of p value) translation (116), translational elongation (65), RNA processing (89), ribonucleoprotein complex biogenesis (46), RNA splicing (56), and ribosome biogenesis (35), suggesting these may also be dependent on pHis signaling. In this regard, His phosphorylation (unlike pSer, pThr, and pTyr) results in a positive to negative charge switch that may help regulate binding of proteins to nucleic acids.

While these pHis mAbs are isoform specific when used for immunoblotting and immunofluorescence, there is significant overlap of proteins (350% or 45%) that bound to the 1-pHis and 3-pHis mAb columns (Tables 1 and S1). We suspect that base-catalyzed isomerization of pHis may occur under the high pH conditions in which the proteomic experiments were performed (Gonzalez-Sanchez et al., 2013). We have made the initial steps toward using these mAbs to study the mammalian pHis proteome; however, there are many other cell lines and tissues to investigate, and further optimization of our pHis mAb immunoaffinity purification and LC-MS/MS methods is necessary to allow the purification of pHis phosphopeptides and direct identification of specific sites of His phosphorylation by MS.

If the mature field of phosphoester phosphorylation is any guide, the nascent and slow-growing field of His phosphorylation will benefit from the development of these immunological reagents and methods, but the development of pHis phosphatase inhibitors and a full accounting of cellular pHis phosphatases, kinases, and substrates are still missing. These mAbs will accelerate progress in all of these areas and help to determine the importance of pHis in human health and disease.

EXPERIMENTAL PROCEDURES

Synthesis of 1-pTza and 3-pTza Peptides and Degenerate Peptide Libraries

Detailed methods for chemical synthesis and analysis of the immunizing pTza peptide libraries can be found in the Supplemental Experimental Procedures. In general, pTza analogs were synthesized by solid-phase peptide synthesis in accordance with published procedures (McAllister and Webb, 2012).

NME and PGAM In Vitro Phosphorylation Assays

In vitro autophosphorylation of purified NME1 and NME2 (10–30 ng/μl) was performed by incubating in TMD buffer (20 mM Tris-HCl [pH 8.0], 5 mM $MgCl_2$, and 1 mM DTT) at room temperature (RT) for 10 min. Reactions were stopped by addition of 5× sample buffer (pH 8.8) and analyzed immediately by modified SDS-PAGE (Supplemental Experimental Procedures). Autophosphorylation of PGAM was performed as described for NME1, except 2,3-DPG was used as the phosphate donor instead of ATP, and incubations were

carried out at 30°C. Reactions lacking ATP or 2,3-DPG or treated briefly with heat or acid served as negative controls. Heat treatment was performed after the addition of 5× sample buffer (pH 8.8) for 10–15 min at 95°C. Acid treatment was performed by adding 25 μl 1 N HCl to a 100 μl reaction and incubating at 37°C for 15 min. Reactions were neutralized with 25 μl 1 N NaOH.

Peptide Dot Blots

Peptide dot blots were used to screen rabbit antisera titer and characterize mAb specificity. The 1-pTza and 3-pTza peptide libraries, His control library, and a pTyr peptide (Nck pY105) were dissolved in water at 1 mg/ml. 1:5 serial dilutions (500, 100, 20, 5, 1, and 0.2 ng/μl) were prepared for each peptide, and 1 μl was spotted on nitrocellulose and allowed to dry for 1–2 hr at RT. Membranes were blocked 1 hr at RT in casein blocking buffer (0.1% casein, 0.2× PBS −/−) and incubated with rabbit antisera (diluted 1:1,000 in blocking buffer with 0.1% Tween 20) for 1 hr at RT or overnight at 4°C. pTza peptide dot blots were also used to characterize pHis mAbs. 1-pTza, 3-pTza, or His was incorporated into synthetic peptides of defined sequences (Supplemental Experimental Procedures) from mammalian proteins with mapped pHis sites (Table 1). Peptides were dissolved in water at 1 mg/ml. 1:5 serial dilutions were prepared and spotted as described above.

Immunofluorescence

Primary murine macrophages were differentiated from bone marrow progenitors (Zhang et al., 2008) plated on coverslips and incubated overnight in fresh medium. Cells were incubated with 10 μg/ml Oregon Green-Dextran 488 and/or LysoTracker (50 nM) for 1–2 hr prior to fixation with 4% paraformaldehyde (PFA) for 10 min. Negative controls were performed by boiling slides for 5–10 min in 0.01 M citrate buffer or by pre-incubation of pHis mAbs with pTza blocking peptides (5 μg/ml). Cells were permeabilized in blocking buffer (PBS, 5% serum [second Ab species], 2% BSA, and 0.1% Tween) with 0.1% Triton X-100 for 1 hr at 4°C. Primary antibodies were diluted to 1 μg/ml in blocking buffer and incubated with slides for 2 hr at 4°C. Slides were washed 5× with cold PBS + 0.1% Tween and incubated with second Ab diluted 1:400 in blocking buffer for 1 hr at 4°C. Slides were mounted on coverslips after washing 5× with cold PBS + 0.1% Tween. See also the Supplemental Experimental Procedures for immunostaining of HeLa cells.

SUPPLEMENTAL INFORMATION

Supplemental Information includes Supplemental Experimental Procedures, six figures, and two tables and can be found with this article online at http://dx.doi.org/10.1016/j.cell.2015.05.046.

AUTHOR CONTRIBUTIONS

S.R.F. conceived of and performed experiments, developed methods and pHis mAb screening assays, characterized mAbs, cultured hybridomas, performed pAb and mAb purification, and wrote the paper. J.M. performed peptide synthesis, assisted with rabbit immunization strategy, and discussed results. A.A. performed pHis mass spectrometry analysis in J.R.Y.'s lab at TSRI. T.H. conceived of degenerate peptide strategy and experiments and edited the manuscript. L.M. performed HeLa and U2OS cell immunofluorescence (IF). A.Z. performed pHis mAb IF experiments on macrophages in G.L.'s lab at Salk. Our collaborators at Sanofi designed and synthesized the pTza peptide libraries; J.M. and A.B. designed pTza peptide library synthesis, J.M., M.S., and F.A.-O. synthesized pTza analogs and peptides. All authors reviewed and commented on the manuscript.

ACKNOWLEDGMENTS

The authors thank Joseph Kim and Ronghua Li at Sanofi for peptide synthesis and William Brondyk (Genzyme) and Jean-Dominique Guitton (Sanofi) for large-scale mAb purification. This work was supported by USPHS grants (CA80100, CA82683, and CA194584) (to T.H.) and made use of the Peptide Synthesis and Biophotonics Cores (supported by P30CA14195). The Helmsley Center for Genomic Medicine also provided support. S.R.F. received funding from an NIH training grant (2 T32 CA009370) and a Salk Institute Innovation Grant. T.H. is a Frank and Else Schilling American Cancer Society Professor and holds the Renato Dulbecco Chair in Cancer Research. A.Z. received support from the Human Frontiers Science Program. L.M. received a Genentech Foundation Fellowship for Cancer Research. G.L. received support from the NIH (R01 NS085296). J.R.Y. received support from an NCRR grant (5P41RR011823-17) and an NIGMS grant (8P41GM103533-17).

Received: October 15, 2014
Revised: March 13, 2015
Accepted: April 20, 2015
Published: July 2, 2015

REFERENCES

Attwood, P.V., Piggott, M.J., Zu, X.L., and Besant, P.G. (2007). Focus on phosphohistidine. Amino Acids *32*, 145–156.

Besant, P.G., and Attwood, P.V. (2012). Histone H4 histidine phosphorylation: kinases, phosphatases, liver regeneration and cancer. Biochem. Soc. Trans. *40*, 290–293.

Boissan, M., Montagnac, G., Shen, Q., Griparic, L., Guitton, J., Romao, M., Sauvonnet, N., Lagache, T., Lascu, I., Raposo, G., et al. (2014). Membrane trafficking. Nucleoside diphosphate kinases fuel dynamin superfamily proteins with GTP for membrane remodeling. Science *344*, 1510–1515.

Boyer, P.D., Deluca, M., Ebner, K.E., Hultquist, D.E., and Peter, J.B. (1962). Identification of phosphohistidine in digests from a probable intermediate of oxidative phosphorylation. J. Biol. Chem. *237*, PC3306–PC3308.

Cai, X., Srivastava, S., Surindran, S., Li, Z., and Skolnik, E.Y. (2014). Regulation of the epithelial Ca^{2+} channel TRPV5 by reversible histidine phosphorylation mediated by NDPK-B and PHPT1. Mol. Biol. Cell *25*, 1244–1250.

Conery, A.R., Sever, S., and Harlow, E. (2010). Nucleoside diphosphate kinase Nm23-H1 regulates chromosomal stability by activating the GTPase dynamin during cytokinesis. Proc. Natl. Acad. Sci. USA *107*, 15461–15466.

Frackelton, A.R., Jr., Ross, A.H., and Eisen, H.N. (1983). Characterization and use of monoclonal antibodies for isolation of phosphotyrosyl proteins from retrovirus-transformed cells and growth factor-stimulated cells. Mol. Cell. Biol. *3*, 1343–1352.

Franceschini, A., Szklarczyk, D., Frankild, S., Kuhn, M., Simonovic, M., Roth, A., Lin, J., Minguez, P., Bork, P., von Mering, C., and Jensen, L.J. (2013). STRING v9.1: protein-protein interaction networks, with increased coverage and integration. Nucleic Acids Res. *41*, D808–D815.

Fraser, M.E., James, M.N.G., Bridger, W.A., and Wolodko, W.T. (2000). Phosphorylated and dephosphorylated structures of pig heart, GTP-specific succinyl-CoA synthetase. J. Mol. Biol. *299*, 1325–1339.

Garin, J., Diez, R., Kieffer, S., Dermine, J.F., Duclos, S., Gagnon, E., Sadoul, R., Rondeau, C., and Desjardins, M. (2001). The phagosome proteome: insight into phagosome functions. J. Cell Biol. *152*, 165–180.

Gold, E.S., Underhill, D.M., Morrissette, N.S., Guo, J., McNiven, M.A., and Aderem, A. (1999). Dynamin 2 is required for phagocytosis in macrophages. J. Exp. Med. *190*, 1849–1856.

Gonzalez-Sanchez, M.B., Lanucara, F., Helm, M., and Eyers, C.E. (2013). Attempting to rewrite history: challenges with the analysis of histidine-phosphorylated peptides. Biochem. Soc. Trans. *41*, 1089–1095.

Hamby, C.V., Abbi, R., Prasad, N., Stauffer, C., Thomson, J., Mendola, C.E., Sidorov, V., and Backer, J.M. (2000). Expression of a catalytically inactive H118Y mutant of nm23-H2 suppresses the metastatic potential of line IV Cl 1 human melanoma cells. Int. J. Cancer *88*, 547–553.

Hartsough, M.T., Morrison, D.K., Salerno, M., Palmieri, D., Ouatas, T., Mair, M., Patrick, J., and Steeg, P.S. (2002). Nm23-H1 metastasis suppressor phosphorylation of kinase suppressor of Ras via a histidine protein kinase pathway. J. Biol. Chem. *277*, 32389–32399.

Huang, W., Sherman, B.T., and Lempicki, R.A. (2009). Systematic and integrative analysis of large gene lists using DAVID bioinformatics resources. Nat. Protoc. *4*, 44–57.

Hunter, T., and Sefton, B.M. (1980). Transforming gene product of Rous sarcoma virus phosphorylates tyrosine. Proc. Natl. Acad. Sci. USA *77*, 1311–1315.

Johnson, P.J., Coussens, P.M., Danko, A.V., and Shalloway, D. (1985). Overexpressed pp60c-src can induce focus formation without complete transformation of NIH 3T3 cells. Mol. Cell. Biol. *5*, 1073–1083.

Kee, J.M., and Muir, T.W. (2012). Chasing phosphohistidine, an elusive sibling in the phosphoamino acid family. ACS Chem. Biol. *7*, 44–51.

Kee, J.M., Villani, B., Carpenter, L.R., and Muir, T.W. (2010). Development of stable phosphohistidine analogues. J. Am. Chem. Soc. *132*, 14327–14329.

Kee, J.M., Oslund, R.C., Perlman, D.H., and Muir, T.W. (2013). A pan-specific antibody for direct detection of protein histidine phosphorylation. Nat. Chem. Biol. *9*, 416–421.

Kee, J.M., Oslund, R.C., Couvillon, A.D., and Muir, T.W. (2015). A second-generation phosphohistidine analog for production of phosphohistidine antibodies. Org. Lett. *17*, 187–189.

Lapek, J.D., Jr., Tombline, G., Kellersberger, K.A., Friedman, M.R., and Friedman, A.E. (2015). Evidence of histidine and aspartic acid phosphorylation in human prostate cancer cells. Naunyn Schmiedebergs Arch. Pharmacol. *388*, 161–173.

Matthews, H. (1995). Protein kinases and phosphatases that act on histidine, lysine, or arginine residues in eukaryotic proteins: a possible regulator of the MAPK cascade. Pharmacol. Ther. *67*, 232–350.

McAllister, T.E., and Webb, M.E. (2012). Triazole phosphohistidine analogues compatible with the Fmoc-strategy. Org. Biomol. Chem. *10*, 4043–4049.

McAllister, T.E., Nix, M.G., and Webb, M.E. (2011). Fmoc-chemistry of a stable phosphohistidine analogue. Chem. Commun. (Camb.) *47*, 1297–1299.

Moréra, S., LeBras, G., Lascu, I., Lacornbe, M.L., Véron, M., and Janin, J. (1994). Refined X-ray structure of Dictyostelium discoideum nucleoside diphosphate kinase at 1.8 A resolution. J. Mol. Biol. *243*, 873–890.

Olsen, J.V., Blagoev, B., Gnad, F., Macek, B., Kumar, C., Mortensen, P., and Mann, M. (2006). Global, in vivo, and site-specific phosphorylation dynamics in signaling networks. Cell *127*, 635–648.

Pesis, K.H., Wei, Y., Lewis, M., and Matthews, H.R. (1988). Phosphohistidine is found in basic nuclear proteins of Physarum polycephalum. FEBS Lett. *239*, 151–154.

Srivastava, S., Li, Z., Ko, K., Choudhury, P., Albaqumi, M., Johnson, A.K., Yan, Y., Backer, J.M., Unutmaz, D., Coetzee, W.A., and Skolnik, E.Y. (2006). Histidine phosphorylation of the potassium channel KCa3.1 by nucleoside diphosphate kinase B is required for activation of KCa3.1 and CD4 T cells. Mol. Cell *24*, 665–675.

Steeg, P.S., Bevilacqua, G., Kopper, L., Thorgeirsson, U.P., Talmadge, J.E., Liotta, L.A., and Sobel, M.E. (1988). Evidence for a novel gene associated with low tumor metastatic potential. J. Natl. Cancer Inst. *80*, 200–204.

Thakur, R.K., Yadav, V.K., Kumar, P., and Chowdhury, S. (2011). Mechanisms of non-metastatic 2 (NME2)-mediated control of metastasis across tumor types. Naunyn Schmiedebergs Arch. Pharmacol. *384*, 397–406.

Tso, P.H., Wang, Y., Yung, L.Y., Tong, Y., Lee, M.M., and Wong, Y.H. (2013). RGS19 inhibits Ras signaling through Nm23H1/2-mediated phosphorylation of the kinase suppressor of Ras. Cell. Signal. *25*, 1064–1074.

Vander Heiden, M.G., Locasale, J.W., Swanson, K.D., Sharfi, H., Heffron, G.J., Amador-Noguez, D., Christofk, H.R., Wagner, G., Rabinowitz, J.D., Asara, J.M., and Cantley, L.C. (2010). Evidence for an alternative glycolytic pathway in rapidly proliferating cells. Science *329*, 1492–1499.

Wagner, P.D., and Vu, N.D. (1995). Phosphorylation of ATP-citrate lyase by nucleoside diphosphate kinase. J. Biol. Chem. *270*, 21758–21764.

Wieland, T., Hippe, H.-J., Ludwig, K., Zhou, X.-B., Korth, M., and Klumpp, S. (2010). Reversible histidine phosphorylation in mammalian cells: a teeter-totter formed by nucleoside diphosphate kinase and protein histidine phosphatase 1. Methods Enzymol. *471*, 379–402.

Zhang, X., Goncalves, R., and Mosser, D.M. (2008). The isolation and characterization of murine macrophages. Curr. Protoc. Immunol. *Chapter 14*, Unit 14.1.